

# Microglial TNF $\alpha$ controls GABA<sub>A</sub>R plasticity, slow waves and memory consolidation during sleep

Maria Joana Pinto<sup>1</sup>, Lucy Bizien<sup>1</sup>, Julie M.J. Fabre<sup>1</sup>, Nina Đukanović<sup>1</sup>, Valentin Lepetz<sup>1</sup>, Fiona Henderson<sup>2</sup>, Marine Pujo<sup>1</sup>, Romain W. Sala<sup>1</sup>, Thibault Tarpin<sup>1</sup>, Daniela Popa<sup>1</sup>, Antoine Triller<sup>1</sup>, Clément Léna<sup>1\*</sup>, Véronique Fabre<sup>2\*</sup>, Alain Bessis<sup>1\*</sup>

## Affiliations :

1-Institut de Biologie de l'École normale supérieure (IBENS), École normale supérieure, CNRS, INSERM, Université PSL, 75005 Paris, France.

2-Neurosciences Paris Seine - Institut de Biologie Paris Seine (NPS - IBPS), CNRS, INSERM, Sorbonne Universités, Paris, France

\*Corresponding authors. Emails: [alain.bessis@bio.ens.psl.eu](mailto:alain.bessis@bio.ens.psl.eu); [clement.len@bio.ens.psl.eu](mailto:clement.len@bio.ens.psl.eu); [veronique.fabre@inserm.fr](mailto:veronique.fabre@inserm.fr)

**ABSTRACT:** Microglia sense the changes in their environment. How microglia actively translate these changes into suitable cues to adapt brain physiology is unknown. We reveal an activity-dependent regulation of cortical inhibitory synapses plasticity by microglia, driven by purinergic signaling acting on P2RX7 and mediated by microglia-derived TNF $\alpha$ . We demonstrate that sleep induces this microglia-dependent inhibitory plasticity by promoting synaptic enrichment of GABA<sub>A</sub>Rs. We further show that in turn, microglia-specific depletion of TNF $\alpha$  alters slow waves during NREM sleep and blunts sleep-dependent memory consolidation. Together, our results reveal that microglia orchestrate sleep-intrinsic plasticity of inhibitory synapses, ultimately sculpting sleep slow waves and memory.

Microglia, the immune cells of the brain, tune neuronal networks in the healthy brain by finely modulating synapses (Kettenmann et al., 2013). They can sculpt developing circuits and remodel neuronal connectivity in adulthood by adjusting synapse density, function and plasticity (Favuzzi et al., 2021; Nguyen et al., 2020; Parkhurst et al., 2013; Schafer et al., 2012; Wang et al., 2020). Microglia accomplish these functions either by direct interaction with synaptic elements (Miyamoto et al., 2016; Schafer et al., 2012) or through the release of factors (Lewitus et al., 2016; Parkhurst et al., 2013). Many of the latter, such as prostaglandin, BDNF, IL-1 $\beta$  or TNF $\alpha$ , control synaptic plasticity and were independently shown to regulate sleep (Porkka-Heiskanen, 2013). Recent work highlights the ability of microglia to control sleep duration (Corsi et al., 2021; Liu et al., 2021); however, whether and how microglia-released factors shape sleep via modulation of synaptic plasticity remains unknown.

Synapse plasticity in the sleeping brain likely supports crucial functions of sleep. In the cortex, spine turnover during sleep is associated to learning and memory (Li et al., 2017; Yang et al., 2014) and, in parallel, wake-associated strengthening of excitatory synapses is downscaled during sleep (Vyazovskiy et al., 2008a; Diering et al., 2017). Synaptic inhibition is critically involved in sleep generation and sleep oscillations (Dixon et al., 2015; Funk et al., 2017; Niethard et al., 2018) but whether and how inhibitory synapses are dynamically modulated during sleep remains poorly understood. Here, we uncover the molecular pathway underlying sleep-intrinsic microglia-dependent modulation of synaptic GABA<sub>AR</sub> as well as its impact on sleep slow waves and sleep-dependent memory consolidation.

### **Daily modulation of GABA<sub>AR</sub>s in a sleep- and microglia-dependent manner**

We first analyzed the modulation of synapses in the frontal cortex across the 24h light/dark cycle by measuring the synaptic content of neurotransmitter receptors (fig. 1 and fig. S1 and S2). Mice sleep more during the light phase and spend most of the dark phase awake. Therefore, we compared brains of mice at Zeitgeber time 18 (ZT18; dark/middle of wake phase) and at ZT6 (light/middle of sleep phase; fig. 1a). We focused on cortical layer 1 (L1) which is a key node for wide-scale cortical computation (Schuman et al., 2021). Consistent with the well-established downscaling of excitatory synapses during sleep (Diering et al., 2017), synaptic accumulation of the AMPA receptor subunit GluA2 was decreased at ZT6 as compared to ZT18 (fig. S1). Yet, analysis of L1 inhibitory synapses revealed an increased enrichment of synaptic, but not extra-synaptic, GABA<sub>AR</sub>- $\gamma$ 2 and - $\alpha$ 1 subunits at ZT6 (fig. 1a-c and fig. S2b-d), as well as an enhanced proportion of inhibitory synapses containing a GABA<sub>AR</sub> cluster (fig. S2e). In contrast, in layer 5 (L5) the synaptic content of GABA<sub>AR</sub> $\gamma$ 2 did not significantly differ between ZT6 and ZT18 (fig. 1e and fig. S2f). These results reveal a novel form of regulation of GABAergic synapses across the light/dark cycle with synaptic enrichment of GABA<sub>AR</sub>s in L1 during the light phase (ZT6), which likely contributes to upregulation of inhibitory transmission in the upper cortex during this phase (Bridi et al., 2020).

To discriminate between a sleep-intrinsic or time of day-dependent regulation of synaptic GABA<sub>AR</sub>, mice were forced to stay awake during their normal sleep period (sleep deprivation from ZT0 to ZT6, SD6; fig. 1a). The synaptic content of GABA<sub>AR</sub> was not different between mice at ZT18 and mice sleep-deprived in the light

phase (SD6; fig. 1d), showing that modulation of synaptic GABA<sub>AR</sub> in L1 is driven by sleep-dependent mechanisms.

We have previously shown that microglia control the accumulation of receptors at inhibitory synapses in the spinal cord (Cantaut-Belarif et al., 2017). This prompted us to investigate the involvement of microglia in the modulation of synaptic GABA<sub>AR</sub> over the sleep/wake cycle. Strikingly, microglia depletion by feeding mice with the CSF1R antagonist PLX3397 (PLX) (Elmore et al., 2014) (fig. S2a, b) completely prevented the changes in synaptic GABA<sub>AR</sub>s content between ZT6 and ZT18 (fig. 1c and fig. S2b,e). This shows that the sleep-dependent modulation of synaptic GABA<sub>AR</sub> in L1 requires microglia.

### Modulation of synaptic GABA<sub>AR</sub> by microglial P2RX7 -TNF $\alpha$ signaling via CaMKII

We next identified the molecular actors of this novel microglia-dependent synaptic regulation (fig. 2), first in an *ex-vivo* system before validating them *in vivo*. During sleep, excitatory synaptic plasticity is triggered by NMDAR-dependent dendritic calcium spikes in L1 (Li et al., 2017). We thus selected an NMDA-induced GABAergic plasticity protocol, known as inhibitory long-term potentiation (iLTP). This form of plasticity, known to drive potentiation of excitatory synapses (Lee et al., 1998), also leads to an upregulation of synaptic GABA<sub>AR</sub>s (Petrini et al., 2014) in pyramidal neurons specifically at somatostatin interneurons inputs (SOM-IN) (Chiu et al., 2018), which are mainly located in L1 (Tremblay et al., 2016) (fig. S3). In agreement with the SOM-IN topographical organization, NMDA-induced iLTP in brain organotypic slices led to specific synaptic enrichment of GABA<sub>AR</sub>s in L1 but not in L5 somatic synapses (fig. 2a, b and fig. S4b-d). This protocol thus mimics *ex-vivo* the synaptic regulations occurring during the sleep/wake cycle so we used it to identify the actors of the L1-restricted sleep-related synaptic enrichment of GABA<sub>AR</sub>s (fig. 1). We further demonstrated that this form of GABA<sub>AR</sub> plasticity was completely abolished when microglia were depleted by PLX (fig. 2a, b and fig. S4a, c). We ruled out possible secondary effects of PLX by showing the same effect upon microglia depletion using Mac1-Saporin (SAP) (fig. S4a) or inactivation using minocycline (fig. 2b).

Microglia produce a broad repertoire of signaling molecules that regulate synaptic function (Kettenmann et al., 2013). TNF $\alpha$ , which is mostly if not exclusively produced by microglia in the brain (Zeisel et al., 2018), controls basal synaptic strength (Santello et al., 2011), neurotransmitter receptors' dynamics and homeostatic synaptic plasticity (Stellwagen and Malenka, 2006). We thus hypothesized that microglial TNF $\alpha$  controls the activity-dependent regulation of synaptic GABA<sub>AR</sub>. Indeed, neutralization of TNF $\alpha$  by specific antibodies (fig. 2c) as well as conditional microglia-specific TNF $\alpha$  depletion (fig. 2d and fig. S5a) prevented the enrichment of synaptic GABA<sub>AR</sub> upon iLTP. Soluble TNF $\alpha$  derives from the cleavage of a membrane form of TNF $\alpha$  by the TNF $\alpha$ -converting enzyme (TACE) (Black et al., 1997). Both forms can signal through TNFR1 whereas TNFR2 is only activated by membrane TNF $\alpha$  (Holbrook et al., 2019). The increase of synaptic GABA<sub>AR</sub>s on iLTP-treated slices was prevented by TAPI-1, a TACE inhibitor, and by a TNFR1- but not by a TNFR2-neutralizing antibody (fig. S5b). Finally, we showed that recombinant TNF $\alpha$  and activation of TNFR1 were sufficient to increase synaptic accumulation of GABA<sub>AR</sub> $\alpha$ 1 (fig. S5c-f). These experiments show that microglial soluble TNF $\alpha$  acting through TNFR1 mediates the activity-dependent regulation of GABA<sub>AR</sub> in L1.

We next identified the signaling pathway between neuron and microglia leading to TNF $\alpha$  release upstream of GABA<sub>AR</sub>s regulation. We first demonstrated that the well-established neuronal CX<sub>3</sub>CL1-microglial CX<sub>3</sub>CR1 signaling, with known roles in synaptic plasticity (Rogers et al., 2011), is not involved (fig. S4e). Microglia behavior is finely tuned by ATP via an array of purinergic receptors (Madry and Attwell, 2015). Microglial cells rapidly react to ATP following the activation of neurons by glutamate and NMDA (Badimon et al., 2020; Dissing-Olesen et al., 2014; Li et al., 2012), and the stimulation of microglial P2RX7 promotes the release of TNF $\alpha$  (Suzuki et al., 2004). We thus investigated whether NMDA-induced release of ATP causes microglia-mediated modulation of synaptic GABA<sub>AR</sub>. Indeed, apyrase, a promoter of ATP hydrolysis, PPADS, a broad P2X antagonist, or A740003, a specific P2RX7 antagonist, prevented the increase of synaptic GABA<sub>AR</sub> upon iLTP (fig. 2e). Moreover, BzATP, a P2RX7 agonist (Surprenant et al., 1996) was sufficient to increase postsynaptic GABA<sub>AR</sub> $\alpha$ 1 in L1 (fig. 2f and fig. S6a,b) but not in L5 (fig. S6c). Of note, BzATP had no effect when microglia were depleted or when TNF $\alpha$  was specifically inactivated in microglia (fig. 2f). Thus, ATP/P2RX7 signaling acts upstream of microglial TNF $\alpha$  release to modulate synaptic accumulation of GABA<sub>AR</sub>.

Finally, we explored the intracellular signaling downstream of microglial TNF $\alpha$ . CaMKII $\alpha$  is a central neuronal mediator of postsynaptic plasticity whose activity is triggered by Ca<sup>2+</sup>/calmodulin and can be prolonged in a Ca<sup>2+</sup>-independent manner by its autophosphorylation at Thr286 (Bayer and Schulman, 2019). Upon iLTP, Thr286-autophosphorylated CaMKII $\alpha$  leads to insertion of GABA<sub>AR</sub>s at synapses (Marsden et al., 2010). We reasoned that TNF $\alpha$  may modulate CaMKII $\alpha$  Thr286-phosphorylation, as observed in non-neuronal cells (Defer et al., 2007). Indeed, Thr286-phosphorylation of CaMKII was increased in L1 upon iLTP (fig. 2g) and this increase was abolished by microglial depletion and by blocking P2RX7 or TNF $\alpha$  signaling (fig. 2h). In agreement, BzATP, which upregulates the synaptic content of GABA<sub>AR</sub>s via a microglial relay, was sufficient to enhance CaMKII Thr286-phosphorylation (fig. 2g, h). The finding that CaMKII Thr286 phosphorylation, and therefore its activity, is gated by microglial TNF $\alpha$  downstream neuronal activity emphasizes a cardinal position of microglia in fine-tuning synapses.

Collectively, our results support a bidirectional neuron-microglia crosstalk underlying activity-driven GABAergic potentiation in L1 (fig. 2i): ATP released downstream neuronal activity activates microglial P2RX7 with concomitant release of TNF $\alpha$  which modulates CaMKII autophosphorylation and thereby enrichment of synaptic GABA<sub>AR</sub>s.

### Sleep-dependent modulation of synaptic GABA<sub>AR</sub> driven by P2RX7 and microglial TNF $\alpha$

Having shown that microglial P2RX7/TNF $\alpha$  pathway controls L1 activity-dependent GABA<sub>AR</sub> plasticity via CaMKII autophosphorylation *ex-vivo*, we examined the involvement of this pathway in sleep-dependent modulation of synaptic GABA<sub>AR</sub> across the light/dark cycle (fig. 1). We first showed that CaMKII Thr286-phosphorylation, but not total CaMKII levels, was increased in L1 at ZT6 (fig. 3a, b and fig. S7a). Notably, such regulation was not found in L5 (fig. S7b). Next, we showed that Thr286-phosphorylation of CaMKII, as well as the synaptic content of GABA<sub>AR</sub>s in L1, were not enhanced at ZT6 in mice with microglia-

specific TNF $\alpha$  depletion (micTNF $\alpha$ -KO, fig. S5a) and in P2rx7-KO mice (fig. 3a-c and fig. S7c, d). This shows that P2RX7 and microglial TNF $\alpha$  drive daily fluctuations in CaMKII Thr286 phosphorylation and are required for sleep-dependent GABA<sub>A</sub>R synaptic upregulation in L1 during the light phase.

### NREM slow waves shaped by microglial TNF $\alpha$

The results above show that microglial TNF $\alpha$  is required for a novel sleep-dependent regulation of inhibitory synapses in cortical L1. Sleep is an alternation of REM and NREM sleep periods which are hallmark by major EEG oscillatory events (Adamantidis et al., 2019). During NREM sleep, slow waves in the delta frequency band (0.1-4Hz), quantified as slow wave activity (SWA), result from the synchronous alternation of active (up) and silent (down) states of cortical neurons. Cortical GABAergic inhibition is a major actor of NREM sleep slow waves (Hay et al., 2021; Lemieux et al., 2015). In particular, the activation of somatostatin positive interneurons, that mainly target L1, triggers down-states (Funk et al., 2017; Niethard et al., 2018). Because microglial TNF $\alpha$  modulates synaptic GABA<sub>A</sub>R at L1 during sleep, we anticipated that it could also shape SWA. Sleep was analyzed using EMG and epidural EEG recordings, and we concentrated our analysis in the frontal cortex where slow waves are predominant (Vyazovskiy et al., 2006). We first showed that microglial TNF $\alpha$  has limited effects on sleep-wake patterns as shown by the lack of major alterations in the amounts of wake, NREM and REM sleep between micTNF $\alpha$ -KO and tCTL mice along a light/dark cycle (fig. 4a). Of note, the daily amount of REM sleep and number of REM bouts was increased on micTNF $\alpha$ -KO (table S1). This phenotype agrees with a suppressive effect of TNF $\alpha$  on REM sleep when injected into the basal forebrain (Terao et al., 1998). We thus anticipate that microglial TNF $\alpha$  may control REM by acting at the basal forebrain, which is out of the scope of this study and therefore not further explored.

We then analysed the spectral density of the EEG during sleep (figure 4b). In agreement with a role of microglial TNF $\alpha$  in the regulation of SWA, we found a shift in the EEG spectral density towards lower frequency activity during NREM sleep with a slower peak frequency in the delta range in micTNF $\alpha$ -KO as compared to tCTL ( $p=0.02539$ ). There were no detectable differences in the other frequency ranges nor in REM sleep (fig. 4b). Finally, we explored how microglial TNF $\alpha$  shapes the properties of individual slow waves during NREM sleep. Slow waves were identified in the epidural EEG as alternation of large transient negative and positive deflections in the 0.1-4 Hz filtered EEG (fig. 4c). We verified that these deflections correspond to up and down states respectively (fig. S8; Nir et al. 2011). Remarkably, the maximum ascending slope of the slow waves, which coincides with the onset of the cortical positive deflection (downstate; fig. S8c), was decreased and the duration of the SW down state (fig. S8a, b) was increased in mice depleted of microglial TNF $\alpha$  as compared to controls (fig. 4d). These results indicate that microglial TNF $\alpha$  shapes slow waves during NREM sleep by favouring transition into the down states.

### Microglial TNF $\alpha$ tunes sleep-dependent memory consolidation.

Slow waves are known to play a causal role for the consolidation of memory during sleep (Fattinger et al., 2017; Marshall et al., 2006). Our previous results show that microglial TNF $\alpha$  exquisitely shapes slow waves during NREM sleep, leading us to anticipate a crucial role of microglial TNF $\alpha$  in the memory consolidation

processes during sleep. To test this hypothesis, we compared the consolidation of a complex motor learning task known to be sleep-dependent (Nagai et al., 2017) in micTNF $\alpha$ -KO and tCTL mice. In this learning paradigm, mice learnt to run on top of a complex wheel attached to an accelerating rotarod in a first 20-trial session (S1). After one day of ad libitum sleep, performance on the complex wheel was assessed on a second 20-trial session by measuring the latency to fall (S2; fig. 5a, b).

We first confirmed that the learning, evaluated as the improvement of performance within each session, was not different between tCTL and micTNF $\alpha$ -KO (fig. 5c). This shows that lack of microglial TNF $\alpha$  did not alter complex motor learning, which is known to be sleep-independent (Nagai et al., 2017). We further showed that it does not impair locomotor activity and does not induce anxiety-like behavior as assessed in an open-field task (fig. S9). We next measured the improvement of performance in the complex motor learning task between S1 and S2 and found that it was higher in tCTL as compared with micTNF $\alpha$ -KO (fig. 5d). Finally, we tested the memory consolidation by comparing performance at the beginning of the second session (First S2) with either the last or the mean performance of the first session (Last S1 or Mean S1). In agreement with our initial hypothesis, memory consolidation was impaired in mice lacking microglial TNF $\alpha$  as compared to controls (fig. 5e). Remarkably, in the complex motor learning task, the improvement of performance between sessions and the memory consolidation are both known to be sleep-dependent processes (Nagai et al., 2017).

## Discussion

Microglia, the principal immune cells of the brain, are now acknowledged as instrumental for the perception of the external environment (Thion et al., 2018). How microglia actively translate their external sensing into suitable cues to adapt circuitries in the healthy brain is yet unknown. Our results favour a model in which microglia sense neuronal activity through an ATP/P2RX7 signalling pathway and respond to it by releasing TNF $\alpha$ . Microglial TNF $\alpha$  then gates the phosphorylation of neuronal CaMKII that modulates GABA<sub>A</sub>R content at cortical synapses (fig. 2). During sleep, this pathway is likely recruited by calcium spikes on apical dendrites of pyramidal neurons (Li et al., 2017), leading to strengthening of inhibitory synapses by upregulation of synaptic GABA<sub>A</sub>R content (figs. 1 and 3). In line with a prominent role of inhibition in the generation of slow waves (Funk et al., 2017; Hay et al., 2021; Lemieux et al., 2015; Niethard et al., 2018; Zucca et al., 2017) microglial TNF $\alpha$  shapes slow waves by controlling transition into down states (fig. 4) and is thereby involved in sleep-dependent memory consolidation (fig. 5).

TNF $\alpha$  has long been known as a sleep factor. Administration of exogenous TNF $\alpha$  promotes SWA and NREM sleep (Fang et al., 1997; Yoshida et al., 2004) whereas inhibition of endogenous TNF $\alpha$  reduces NREM sleep (refs in Rockstrom et al., 2018). This is in apparent contradiction with our results showing no difference in NREM sleep amount in mice with microglia-specific TNF $\alpha$  depletion. Yet, to increase NREM sleep, TNF $\alpha$  was injected either directly in the brain (Yoshida et al., 2004) or intraperitoneally (Fang et al., 1997) at concentrations probably higher than the physiological concentration (Garré et al., 2017), with putative widespread diffusion and off-target and indirect effects. Finally, the studies using TNF $\alpha$  knock-out have not used cell specific and inducible inactivation and it is thus difficult to discriminate between microglial specific effect to indirect effects due non-microglial TNF $\alpha$  and/or secondary developmental alterations. Finally, TNF $\alpha$  is also a major mediator of inflammation, which induces sleep dysfunction by yet elusive mechanisms (Irwin, 2019). Our work now provides possible molecular and cellular links between sleep and inflammation.

Our results were obtained from experiments performed both *in vivo* and in organotypic slices. The latter system closely mimics the *in vivo* brain by preserving tissue architecture and cellular composition. In these slices microglia retain their 3D ramified morphology and their functional properties (De Simoni et al., 2008; Delbridge et al., 2020; Weinhard et al., 2018). They further conserve their ability to regulate synapses (Cantaut-Belarif et al., 2017; Pascual et al., 2012). This indicates that functional interactions between neurons and microglia are conserved in organotypic slices. Indeed, in this work, we have identified microglial TNF $\alpha$ , ATP/P2RX7 and CaMKII as molecular actors of synaptic GABA<sub>A</sub>Rs regulation in organotypic slices and we have further confirmed their role *in vivo* in the regulation of GABA<sub>A</sub>Rs plasticity during the sleep/wake cycle.

Excitatory synapses are scaled down during sleep, through removal of AMPA receptors, to compensate for potentiation due to ongoing learning during wake (Vyazovskiy et al., 2008a). Microglia contribute to downscaling during sleep by eliminating excitatory synapses (Choudhury et al., 2019), a behaviour presumably tuned down during wake by noradrenaline (Liu et al., 2019; Stowell et al., 2019). More recently, microglial CX3CR1 signalling was shown to differentially regulate excitatory synaptic transmission along the light/dark cycle (Corsi et al., 2021). We now show that microglia tune a sleep/wake regulation of inhibitory synapses

restricted to cortical layer 1, via mobilization of the P2RX7/TNF $\alpha$  signalling and regulation of synaptic GABA<sub>A</sub>R content. Altogether, microglia are arising as active players in excitatory and inhibitory synapse remodelling along the sleep/wake cycle, likely to underlie daily oscillations in synaptic strength (Bridi et al., 2020; Tononi and Cirelli, 2019; Vyazovskiy et al., 2008b).

Cortical inhibition is involved in the control of slow wave activity during NREM sleep (Funk et al., 2017; Zucca et al., 2017; Zielinski et al., 2019), with a prominent role in the onset of down states (Chen et al., 2012; Lemieux et al., 2015). Such control is likely achieved through a combination of different inhibitory networks. Thalamic drive onto L1 inhibitory neurogliaform cells induces transition into down states (Hay et al., 2021). In addition, SOM-IN firing precedes entry into down states (Niethard et al., 2018) and accordingly their stimulation increases the slope of slow waves and triggers down-states (Funk et al., 2017). We now show that in agreement with their ability to modulate inhibitory synapses in the upper layers of the cortex, microglia are genuine regulators of slow waves during NREM sleep. Together with evidence of astrocytic involvement in slow wave activity (Szabó et al., 2017; Vaidyanathan et al., 2021), our work offers insight into how local glial modulation of neuronal networks tunes brain oscillations during sleep. One of the major physiological role of sleep is to allow memory consolidation (Klinzing et al., 2019), which critically depends on slow waves (Fattinger et al., 2017; Marshall et al., 2006). We now demonstrated that mice lacking TNF $\alpha$  display weaker consolidation than control mice, a process that putatively relies on the molecular microglia-neuron signaling herein described and downstream impact on neuronal dynamics during NREM sleep.

Finally, this work adds to the yet limited knowledge of microglia functions in the healthy adult brain (Parkhurst et al., 2013; Wang et al., 2020) and establishes microglia as genuine regulators of inhibitory synapses plasticity, brain oscillations and memory in the healthy brain. Noteworthy, microglial regulation likely occurs through the control of CaMKII $\alpha$ , which is a cardinal regulator of synaptic plasticity (Bayer and Schulman, 2019). It occurs on SOM interneurons inputs, which are involved in the control of complex behaviours such as sleep, but also decision making and learning (Adler et al., 2019). Finally, this work demonstrates that microglia tune slow waves and support memory consolidation during sleep (Klinzing et al., 2019). We anticipate a far wider involvement of microglia in other forms of plasticity and higher brain functions.

## References

Adamantidis, A.R., Gutierrez Herrera, C., and Gent, T.C. (2019). Oscillating circuitries in the sleeping brain. *Nat. Rev. Neurosci.* *20*, 746–762.

Adler, A., Zhao, R., Shin, M.E., Yasuda, R., and Gan, W.-B. (2019). Somatostatin-Expressing Interneurons Enable and Maintain Learning-Dependent Sequential Activation of Pyramidal Neurons. *Neuron* *102*, 202–216.e7.

Badimon, A., Strasburger, H.J., Ayata, P., Chen, X., Nair, A., Ikegami, A., Hwang, P., Chan, A.T., Graves, S.M., Uweru, J.O., et al. (2020). Negative feedback control of neuronal activity by microglia. *Nature* *586*, 417–423.

Bayer, K.U., and Schulman, H. (2019). CaM Kinase: Still Inspiring at 40. *Neuron* *103*, 380–394.

Black, R.A., Rauch, C.T., Kozlosky, C.J., Peschon, J.J., Slack, J.L., Wolfson, M.F., Castner, B.J., Stocking, K.L., Reddy, P., Srinivasan, S., et al. (1997). A metalloproteinase disintegrin that releases tumour-necrosis factor-alpha from cells. *Nature* *385*, 729–733.

Bridi, M.C.D., Zong, F.-J., Min, X., Luo, N., Tran, T., Qiu, J., Severin, D., Zhang, X.-T., Wang, G., Zhu, Z.-J., et al. (2020). Daily Oscillation of the Excitation-Inhibition Balance in Visual Cortical Circuits. *Neuron* *105*, 621–629.e4.

Cantaut-Belarif, Y., Antri, M., Pizzarelli, R., Colasse, S., Vaccari, I., Soares, S., Renner, M., Dalle, R., Triller, A., and Bessis, A. (2017). Microglia control the glycinergic but not the GABAergic synapses via prostaglandin E2 in the spinal cord. *J. Cell Biol.* *216*, 2979–2989.

Chen, J.-Y., Chauvette, S., Skorheim, S., Timofeev, I., and Bazhenov, M. (2012). Interneuron-mediated inhibition synchronizes neuronal activity during slow oscillation. *J. Physiol.* *590*, 3987–4010.

Chiu, C.Q., Martenson, J.S., Yamazaki, M., Natsume, R., Sakimura, K., Tomita, S., Tavalin, S.J., and Higley, M.J. (2018). Input-Specific NMDAR-Dependent Potentiation of Dendritic GABAergic Inhibition. *Neuron* *97*, 368–377.e3.

Choudhury, M.E., Miyanishi, K., Takeda, H., Islam, A., Matsuoka, N., Kubo, M., Matsumoto, S., Kunieda, T., Nomoto, M., Yano, H., et al. (2019). Phagocytic elimination of synapses by microglia during sleep. *Glia* *1*–16.

Corsi, G., Picard, K., Castro, M.A., Garofalo, S., Tucci, F., Chece, G., Percio, C., Golia, M.T., Raspa, M., Scavizzi, F., et al. (2021). Microglia modulate hippocampal synaptic transmission and sleep duration along the light/dark cycle. *Glia* *24*090.

De Simoni, A., Allen, N.J., and Attwell, D. (2008). Charge compensation for NADPH oxidase activity in microglia in rat brain slices does not involve a proton current. *Eur. J. Neurosci.* *28*, 1146–1156.

Defer, N., Azroyan, A., Pecker, F., and Pavoine, C. (2007). TNFR1 and TNFR2 signaling interplay in cardiac myocytes. *J. Biol. Chem.* *282*, 35564–35573.

Delbridge, A.R.D., Huh, D., Brickelmaier, M., Burns, J.C., Roberts, C., Challa, R., Raymond, N., Cullen, P., Carlile, T.M., Ennis, K.A., et al. (2020). Organotypic Brain Slice Culture Microglia Exhibit Molecular Similarity to Acutely-Isolated Adult Microglia and Provide a Platform to Study Neuroinflammation. *Front. Cell. Neurosci.* *14*, 592005.

Diering, G.H., Nirujogi, R.S., Roth, R.H., Worley, P.F., Pandey, A., and Huganir, R.L. (2017). Homer1a drives homeostatic scaling-down of excitatory synapses during sleep. *Science* *355*, 511–515.

Dissing-Olesen, L., LeDue, J.M., Rungta, R.L., Hefendehl, J.K., Choi, H.B., and MacVicar, B.A. (2014). Activation of Neuronal NMDA Receptors Triggers Transient ATP-Mediated Microglial Process Outgrowth. *J. Neurosci.* *34*, 10511–10527.

Dixon, C.L., Harrison, N.L., Lynch, J.W., and Keramidas, A. (2015). Zolpidem and eszopiclone prime  $\alpha 1\beta 2\gamma 2$  GABA<sub>A</sub> receptors for longer duration of activity. *Br. J. Pharmacol.* *172*, 3522–3536.

Elmore, M.R.P., Najafi, A.R., Koike, M.A., Dagher, N.N., Spangenberg, E.E., Rice, R.A., Kitazawa, M., Matusow, B., Nguyen, H., West, B.L., et al. (2014). Colony-stimulating factor 1 receptor signaling is necessary for microglia viability, unmasking a microglia progenitor cell in the adult brain. *Neuron* *82*, 380–397.

Fang, J., Wang, Y., and Krueger, J.M. (1997). Mice lacking the TNF 55 kDa receptor fail to sleep more after TNFalpha treatment. *J. Neurosci. Off. J. Soc. Neurosci.* *17*, 5949–5955.

Fattinger, S., de Beukelaar, T.T., Ruddy, K.L., Volk, C., Heyse, N.C., Herbst, J.A., Hahnloser, R.H.R., Wenderoth, N., and Huber, R. (2017). Deep sleep maintains learning efficiency of the human brain. *Nat. Commun.* *8*, 15405.

Favuzzi, E., Huang, S., Saldi, G.A., Binan, L., Ibrahim, L.A., Fernández-Otero, M., Cao, Y., Zeine, A., Sefah, A., Zheng, K., et al. (2021). GABA-receptive microglia selectively sculpt developing inhibitory circuits. *Cell* *184*, 4048–4063.e32.

Funk, C.M., Peelman, K., Bellesi, M., Marshall, W., Cirelli, C., and Tononi, G. (2017). Role of somatostatin-

positive cortical interneurons in the generation of sleep slow waves. *J. Neurosci.* 1303–1317.

Garré, J.M., Silva, H.M., Lafaille, J.J., and Yang, G. (2017). CX3CR1+ monocytes modulate learning and learning-dependent dendritic spine remodeling via TNF- $\alpha$ . *Nat. Med.* 23, 714–722.

Hay, Y.A., Deperrois, N., Fuchsberger, T., Quarrell, T.M., Koerling, A.-L., and Paulsen, O. (2021). Thalamus mediates neocortical Down state transition via GABAB-receptor-targeting interneurons. *Neuron* 109, 2682–2690.e5.

Holbrook, J., Lara-Reyna, S., Jarosz-Griffiths, H., and McDermott, M. (2019). Tumour necrosis factor signalling in health and disease [version 1; referees: 2 approved]. *F1000Research* 8.

Irwin, M.R. (2019). Sleep and inflammation: partners in sickness and in health. *Nat. Rev. Immunol.*

Kettenmann, H., Kirchhoff, F., and Verkhratsky, A. (2013). Microglia: new roles for the synaptic stripper. *Neuron* 77, 10–18.

Klinzing, J.G., Niethard, N., and Born, J. (2019). Mechanisms of systems memory consolidation during sleep. *Nat. Neurosci.* 22, 1598–1610.

Lee, H.-K., Kameyama, K., Huganir, R.L., and Bear, M.F. (1998). NMDA Induces Long-Term Synaptic Depression and Dephosphorylation of the GluR1 Subunit of AMPA Receptors in Hippocampus. *Neuron* 21, 1151–1162.

Lemieux, M., Chauvette, S., and Timofeev, I. (2015). Neocortical inhibitory activities and long-range afferents contribute to the synchronous onset of silent states of the neocortical slow oscillation. *J. Neurophysiol.* 113, 768–779.

Lewitus, G.M., Konefal, S.C., Greenhalgh, A.D., Pribiag, H., Augereau, K., and Stellwagen, D. (2016). Microglial TNF- $\alpha$  Suppresses Cocaine-Induced Plasticity and Behavioral Sensitization. *Neuron* 90, 483–491.

Li, W., Ma, L., Yang, G., and Gan, W.-B. (2017). REM sleep selectively prunes and maintains new synapses in development and learning. *Nat. Neurosci.* 20, 427–437.

Li, Y., Du, X., Liu, C., Wen, Z., and Du, J. (2012). Reciprocal Regulation between Resting Microglial Dynamics and Neuronal Activity In Vivo. *Dev. Cell* 23, 1189–1202.

Liu, H., Wang, X., Chen, L., Chen, L., Tsirka, S.E., Ge, S., and Xiong, Q. (2021). Microglia modulate stable wakefulness via the thalamic reticular nucleus in mice. *Nat. Commun.* 12, 4646.

Liu, Y.U., Ying, Y., Li, Y., Eyo, U.B., Chen, T., Zheng, J., Umpierre, A.D., Zhu, J., Bosco, D.B., Dong, H., et al. (2019). Neuronal network activity controls microglial process surveillance in awake mice via norepinephrine signaling. *Nat. Neurosci.* 22, 1771–1781.

Madry, C., and Attwell, D. (2015). Receptors, Ion Channels and Signaling Mechanisms Underlying Microglial Dynamics. *J. Biol. Chem.*

Marsden, K.C., Shemesh, A., Bayer, K.U., and Carroll, R.C. (2010). Selective translocation of Ca2+/calmodulin protein kinase II $\alpha$  (CaMKII $\alpha$ ) to inhibitory synapses. *Proc. Natl. Acad. Sci. U. S. A.* 107, 20559–20564.

Marshall, L., Helgadóttir, H., Mölle, M., and Born, J. (2006). Boosting slow oscillations during sleep potentiates memory. *Nature* 444, 610–613.

Miyamoto, A., Wake, H., Ishikawa, A.W., Eto, K., Shibata, K., Murakoshi, H., Koizumi, S., Moorhouse, A.J., Yoshimura, Y., and Nabekura, J. (2016). Microglia contact induces synapse formation in developing somatosensory cortex. *Nat. Commun.* 7, 12540.

Nagai, H., de Vivo, L., Bellesi, M., Ghilardi, M.F., Tononi, G., and Cirelli, C. (2017). Sleep Consolidates Motor Learning of Complex Movement Sequences in Mice. *Sleep* 40.

Nguyen, P.T., Dorman, L.C., Pan, S., Vainchtein, I.D., Han, R.T., Nakao-Inoue, H., Taloma, S.E., Barron, J.J., Molofsky, A.B., Kheirbek, M.A., et al. (2020). Microglial Remodeling of the Extracellular Matrix Promotes Synapse Plasticity. *Cell* 182, 388–403.e15.

Niethard, N., Ngo, H.-V.V., Ehrlich, I., and Born, J. (2018). Cortical circuit activity underlying sleep slow oscillations and spindles. *Proc. Natl. Acad. Sci.* 115, E9220–E9229.

Parkhurst, C.N., Yang, G., Ninan, I., Savas, J.N., Yates, J.R., Lafaille, J.J., Hempstead, B.L., Littman, D.R., and Gan, W.-B. (2013). Microglia promote learning-dependent synapse formation through brain-derived neurotrophic factor. *Cell* 155, 1596–1609.

Pascual, O., Achour, S.B., Rostaing, P., Triller, A., and Bessis, A. (2012). Microglia activation triggers astrocyte-mediated modulation of excitatory neurotransmission. *Proc Natl Acad Sci USA* 109, E197–205.

Petrini, E.M., Ravasenga, T., Hausrat, T.J., Iurilli, G., Olcese, U., Racine, V., Sibarita, J.-B., Jacob, T.C., Moss, S.J., Benfenati, F., et al. (2014). Synaptic recruitment of gephyrin regulates surface GABA(A) receptor dynamics for the expression of inhibitory LTP. *Nat. Commun.* 5, 3921.

Porkka-Heiskanen, T. (2013). Sleep homeostasis. *Curr. Opin. Neurobiol.* 23, 799–805.

Rockstrom, M.D., Chen, L., Taishi, P., Nguyen, J.T., Gibbons, C.M., Veasey, S.C., and Krueger, J.M. (2018).

Tumor necrosis factor alpha in sleep regulation. *Sleep Med. Rev.* *40*, 69–78.

Rogers, J.T., Morganti, J.M., Bachstetter, A.D., Hudson, C.E., Peters, M.M., Grimmig, B. a., Weeber, E.J., Bickford, P.C., and Gemma, C. (2011). CX3CR1 Deficiency Leads to Impairment of Hippocampal Cognitive Function and Synaptic Plasticity. *J. Neurosci.* *31*, 16241–16250.

Santello, M., Bezzi, P., and Volterra, A. (2011). TNF $\alpha$  Controls Glutamatergic Gliotransmission in the Hippocampal Dentate Gyrus. *Neuron* *69*, 988–1001.

Schafer, D., Lehrman, E., Kautzman, A., Koyama, R., Mardinly, A., Yamasaki, R., Ransohoff, R., Greenberg, M., Barres, B., and Stevens, B. (2012). Microglia sculpt postnatal neural circuits in an activity and complement-dependent manner. *Neuron* *74*, 691–705.

Schuman, B., Dellal, S., Prönneke, A., Machold, R., and Rudy, B. (2021). Neocortical Layer 1: An Elegant Solution to Top-Down and Bottom-Up Integration. *Annu. Rev. Neurosci.*

Stellwagen, D., and Malenka, R.C. (2006). Synaptic scaling mediated by glial TNF- $\alpha$ . *Nature* *440*, 1054–1059.

Stowell, R.D., Sipe, G.O., Dawes, R.P., Batchelor, H.N., Lordy, K.A., Whitelaw, B.S., Stoessel, M.B., Bidlack, J.M., Brown, E., Sur, M., et al. (2019). Noradrenergic signaling in the wakeful state inhibits microglial surveillance and synaptic plasticity in the mouse visual cortex. *Nat. Neurosci.* *22*, 1782–1792.

Surprenant, A., Rassendren, F., Kawashima, E., North, R.A., and Buell, G. (1996). The cytolytic P2Z receptor for extracellular ATP identified as a P2X receptor (P2X7). *Science* *272*, 735–738.

Suzuki, T., Hide, I., Ido, K., Kohsaka, S., Inoue, K., and Nakata, Y. (2004). Production and release of neuroprotective tumor necrosis factor by P2X7 receptor-activated microglia. *J. Neurosci. Off. J. Soc. Neurosci.* *24*, 1–7.

Szabó, Z., Héja, L., Szalay, G., Kékesi, O., Füredi, A., Szébényi, K., Dobolyi, Á., Orbán, T.I., Kolacsek, O., Tompa, T., et al. (2017). Extensive astrocyte synchronization advances neuronal coupling in slow wave activity in vivo. *Sci. Rep.* *7*, 6018.

Terao, A., Matsumura, H., Yoneda, H., and Saito, M. (1998). Enhancement of slow-wave sleep by tumor necrosis factor-alpha is mediated by cyclooxygenase-2 in rats. *Neuroreport* *9*, 3791–3796.

Thion, M.S., Ginhoux, F., and Garel, S. (2018). Microglia and early brain development: An intimate journey. *Science* *362*, 185–189.

Tononi, G., and Cirelli, C. (2019). Sleep and synaptic down-selection. *Eur. J. Neurosci.*

Tremblay, R., Lee, S., and Rudy, B. (2016). GABAergic Interneurons in the Neocortex: From Cellular Properties to Circuits. *Neuron* *91*, 260–292.

Vaidyanathan, T.V., Collard, M., Yokoyama, S., Reitman, M.E., and Poskanzer, K.E. (2021). Cortical astrocytes independently regulate sleep depth and duration via separate GPCR pathways. *ELife* *10*, e63329.

Vyazovskiy, V. V., Cirelli, C., Pfister-Genskow, M., Faraguna, U., and Tononi, G. (2008a). Molecular and electrophysiological evidence for net synaptic potentiation in wake and depression in sleep. *Nat. Neurosci.* *11*, 200–208.

Vyazovskiy, V.V., Ruijgrok, G., Deboer, T., and Tobler, I. (2006). Running Wheel Accessibility Affects the Regional Electroencephalogram during Sleep in Mice. *Cereb. Cortex* *16*, 328–336.

Vyazovskiy, V.V., Cirelli, C., Pfister-Genskow, M., Faraguna, U., and Tononi, G. (2008b). Molecular and electrophysiological evidence for net synaptic potentiation in wake and depression in sleep. *Nat. Neurosci.* *11*, 200–208.

Wang, C., Yue, H., Hu, Z., Shen, Y., Ma, J., Li, J., Wang, X.-D., Wang, L., Sun, B., Shi, P., et al. (2020). Microglia mediate forgetting via complement-dependent synaptic elimination. *Science* *367*, 688–694.

Weinhard, L., di Bartolomei, G., Bolasco, G., Machado, P., Schieber, N.L., Neniskyte, U., Exiga, M., Vadisiute, A., Raggioli, A., Schertel, A., et al. (2018). Microglia remodel synapses by presynaptic trogocytosis and spine head filopodia induction. *Nat. Commun.* *9*.

Yang, G., Lai, C.S.W., Cichon, J., Ma, L., Li, W., and Gan, W.-B. (2014). Sleep promotes branch-specific formation of dendritic spines after learning. *Science* *344*, 1173–1178.

Yoshida, H., Peterfi, Z., García-García, F., Kirkpatrick, R., Yasuda, T., and Krueger, J.M. (2004). State-specific asymmetries in EEG slow wave activity induced by local application of TNF $\alpha$ . *Brain Res.* *1009*, 129–136.

Zeisel, A., Hochgerner, H., Lönnerberg, P., Johnsson, A., Memic, F., van der Zwan, J., Häring, M., Braun, E., Borm, L.E., La Manno, G., et al. (2018). Molecular Architecture of the Mouse Nervous System. *Cell* *174*, 999–1014.e22.

Zielinski, M.R., Atochin, D.N., McNally, J.M., McKenna, J.T., Huang, P.L., Strecker, R.E., and Gerashchenko, D. (2019). Somatostatin+/nNOS+ neurons are involved in delta electroencephalogram activity and cortical-dependent recognition memory. *Sleep* *42*.

Zucca, S., D'Urso, G., Pasquale, V., Vecchia, D., Pica, G., Bovetti, S., Moretti, C., Varani, S., Molano-Mazón,

M., Chiappalone, M., et al. (2017). An inhibitory gate for state transition in cortex. *ELife* 6.

### **Acknowledgments:**

This work was funded by : Agence nationale pour la recherche : SYNTRACK -R17096DJ (AT); Agence nationale pour la recherche: EXPECT 17-CE37-0022-2 (CL, DP); European Research Council : PLASTINHIB Project No: 322821 and MICROCOPS (AT); Human Brain Project : HBP SGA2-OPE-2018-0017 (AT); EMBO fellowship: ALTF 362-2017 (MJP);

We gratefully acknowledge Astou Tangara, Benjamin Mathieu and the IBENS imaging facility (IMACHEM-IBiSA), member of the French National Research Infrastructure France-BioImaging (ANR-10-INBS-04), which received support from the "Fédération pour la Recherche sur le Cerveau - Rotary International France" (2011) and from the program « Investissements d'Avenir » ANR-10-LABX-54 MEMOLIFE.

We are grateful to Amandine Delecourt, Eleonore Touzalin, Deborah Souchet for excellent technical assistance.

We thank Sonia Garel (IBENS, Paris), Etienne Audinat (Institut de génomique fonctionnelle, Montpellier) and Lauriane Ulmann and François Rassendren (Institut de génomique fonctionnelle, Montpellier) for providing CX<sub>3</sub>CR1<sup>CreERT2</sup> and Ai9 ; TNF<sup>fl/fl</sup> and P2rx7 -KOs respectively.

We thank the IBPS Behavioral Core Facility for excellent technical assistance.

**Author contributions:** Conceptualization: AB, AT, CL, DP, MJP, VF. Formal Analysis: CL, MJP, VF. Funding acquisition: AB, AT, CL, DP, VF. Investigation: JF, FH, LB, MJP, ND, VF, AB, MP, RWS, TT. Software: CL, VL, MJP. Writing – original draft: AB, MJP. Writing – review & editing: AB, AT, CL, DP, MJP, VF, RWS.

Authors declare that they have no competing interests.

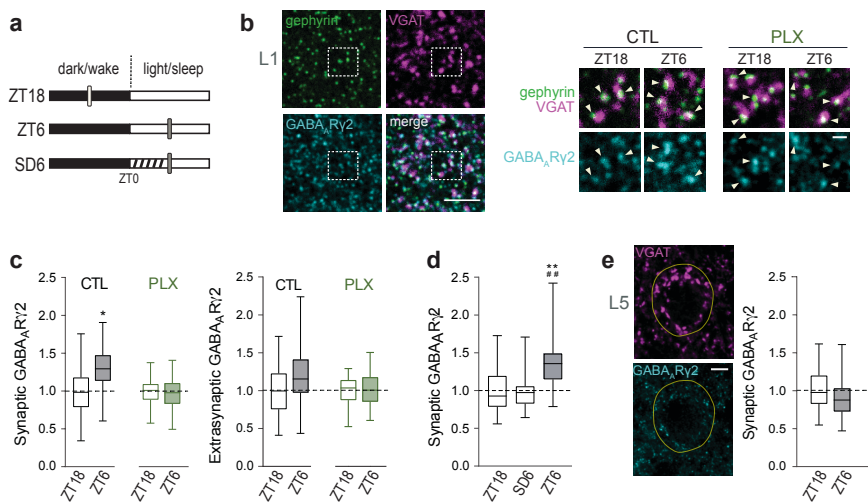


**Fig. 1 –Plasticity of GABA<sub>A</sub>R in the light/dark cycle is sleep- and microglia-dependent. a**, Experimental groups: mice at dark phase (ZT18), mice at light phase (ZT6) and mice submitted to sleep deprivation (dashed) in the light phase (SD6). Vertical bars: time of perfusion. **b**, Representative images showing enrichment of GABA<sub>A</sub>Ry2 (cyan) at cortical L1 inhibitory synapses in the light phase (ZT6). Arrowheads: GABA<sub>A</sub>Ry2 clusters at gephyrin<sup>+</sup>VGAT<sup>+</sup> synapses in control (CTL) or PLX3397-treated mice (PLX). Scale bars, 5 and 1  $\mu$ m. Dashed box corresponds to CTL at ZT18. **c, d**, Mean intensity of GABA<sub>A</sub>Ry2 clusters at gephyrin<sup>+</sup>VGAT<sup>+</sup> synapses (synaptic) and at extrasynaptic sites normalized to ZT18. n= 48 to 65 fields of view (FOVs) from 4-5 mice per group. \*p<0.05, nested t-test; \*\*p<0.01 compared with ZT18 and #p<0.01 compared with SD6, nested one-way ANOVA followed by Sidak's multiple comparison test. **e**, Left: Representative confocal images of VGAT and GABA<sub>A</sub>Ry2 in cortical L5. Yellow line delineates soma identified by NeuN staining. Scale bar, 5  $\mu$ m. Right: Mean intensity of GABA<sub>A</sub>Ry2 at somatic VGAT<sup>+</sup> clusters in L5 normalized to ZT18. n= 60 FOVs from 5 mice per group.

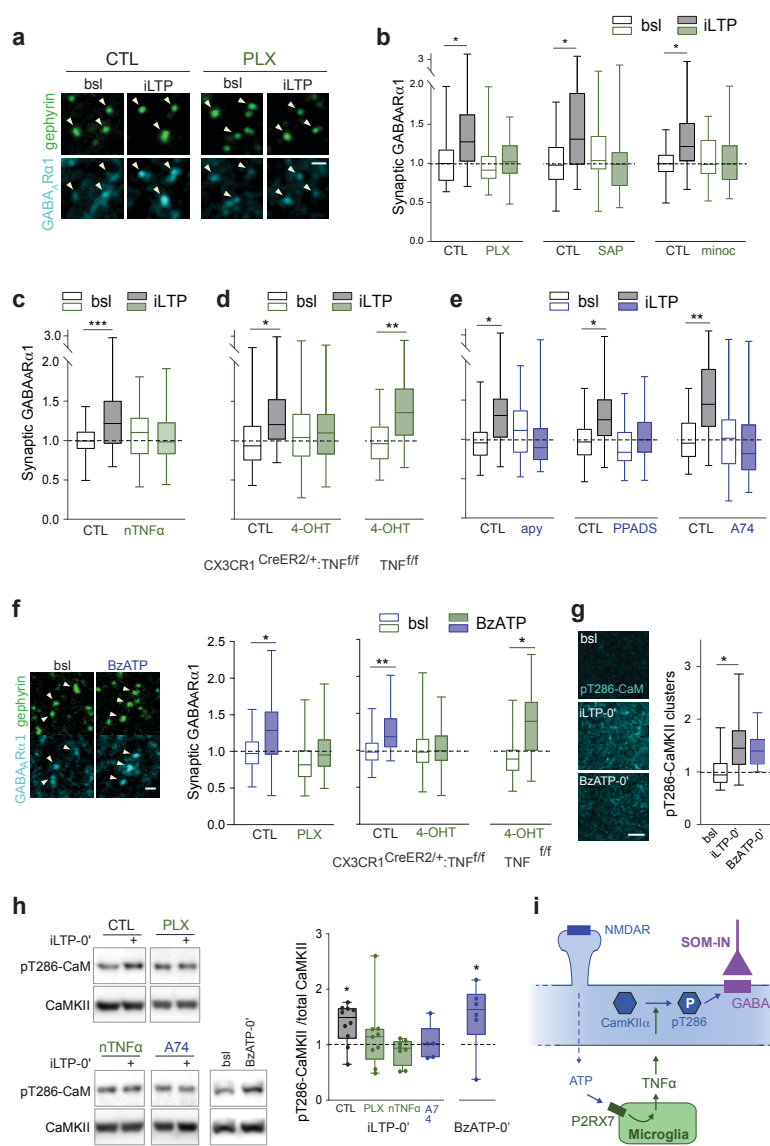


**Fig. 2 – Microglial P2X7R-TNF $\alpha$  signaling drives GABA<sub>A</sub>R $\alpha$  synaptic enrichment through CaMKII $\alpha$  phosphorylation.**

**a**, Representative confocal images showing increase of GABA<sub>A</sub>R $\alpha$ 1 (cyan) at gephyrin $^+$  clusters (arrowheads) upon NMDA-induced inhibitory long-term potentiation (iLTP: 2 min 20  $\mu$ M NMDA/10  $\mu$ M CNQX plus 20 min recovery) in organotypic slices cortical L1 (CTL: control; bsl: baseline). **b-e**, Mean intensity of GABA<sub>A</sub>R $\alpha$ 1 clusters at gephyrin $^+$  cluster normalized to CTL at bsl. n= FOVs/ independent experiments: (b) n= 44 to 69/ 5 to 6; (c) n= 47 to 53/ 5; (d) n= 66 to 102/ 5 to 7; (e) n= 49 to 68/ 7 to 9. \*p<0.05, \*\*p<0.01 and \*\*\*p<0.001, nested one-way ANOVA followed by Sidak's multiple comparison test. iLTP-induced synaptic GABA<sub>A</sub>R enrichment is abolished by: **b**, microglia depletion/inactivation (PLX: PLX3397; SAP: Mac1-saporin; minoc: minocycline); **c**, neutralization of TNF $\alpha$  (nTNF $\alpha$ ); **d**, microglia-specific TNF $\alpha$  deletion through 4-hydroxy-tamoxifen (4-OHT)-induced recombination on CX3CR1<sup>CreERT2/+</sup>:TNF $^{ff}$  but not on a TNF $^{ff}$  background; **e**, ATP hydrolysis (apy), P2XR antagonist (PPADS) and P2X7R antagonist (A74). **f**, Left: Confocal images of GABA<sub>A</sub>R $\alpha$ 1 (cyan) at gephyrin $^+$  clusters (arrowheads) in bsl and upon BzATP treatment. Right: Mean intensity of GABA<sub>A</sub>R $\alpha$ 1 clusters at gephyrin $^+$  clusters normalized to CTL at bsl. n= 49 to 63/ 5 to 6. \*p<0.05, \*\*p<0.01, nested one-way ANOVA followed by Sidak's multiple comparison test. **g**, Left: Thr286-phosphorylated CaMKII is enhanced in L1 at the induction phase of plasticity (iLTP-0' or BzATP-0'). Scale bar, 5  $\mu$ m. Right: Mean intensity of Thr286-phosphorylated CaMKII puncta normalized to bsl. n= 25 to 33 FOVs from 3 independent experiments. \*p<0.05, nested t-test. **h**, Left: Western blot analysis showing iLTP-0'-induced CaMKII Thr286-phosphorylation. Right: Ratio between Thr286-phosphorylated CaMKII and total CaMKII normalized to the respective iLTP-free control. n= 5 to 9 independent experiments. \*p<0.05 compared with respective control, Kruskal-Wallis test followed by Dunn's multiple comparisons test. **i**, Model. ATP released downstream NMDA-induced neuronal activity activates microglial P2RX7, which triggers the release of microglial TNF $\alpha$ . TNF $\alpha$  signaling gates CaMKII $\alpha$  autophosphorylation which controls the enrichment of synaptic GABA<sub>A</sub>R $\alpha$ s in pyramidal neurons.

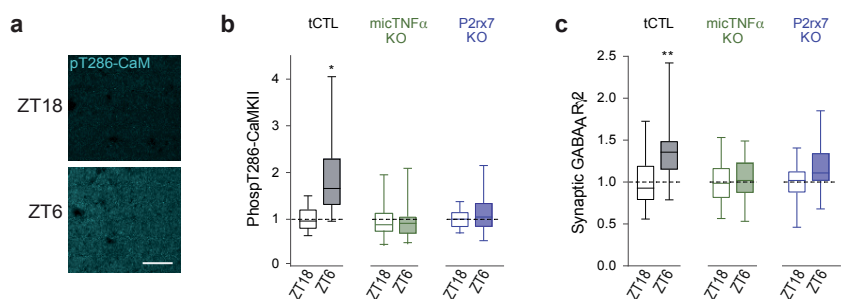


**Fig. 3 – P2RX7 and microglial TNF $\alpha$  promote daily changes in synaptic GABA $_A$  R content and CaMKII phosphorylation.** **a**, Representative confocal images of Thr286-phosphorylated CaMKII immunoreactivity in L1 showing higher intensity at ZT6 than ZT18 in transgenic control mice (tCTL). Scale bar, 20  $\mu$ m. **b**, Mean intensity of Thr286-phosphorylated CaMKII signal in L1 normalized to ZT18 for tCTL, microglia-specific TNF $\alpha$  depletion (micTNF $\alpha$ -KO) and P2rx7-KO mice. n= 37 to 50 FOVs from 4-5 mice per group. **c**, Mean intensity of GABA $_A$ R $\gamma$ 2 clusters at gephyrin $^+$ VGAT $^+$  synapses normalized to ZT18. n= 48 to 65 FOVs from 4-5 mice per group. \*p<0.05 and \*\*p<0.01, nested t-test.

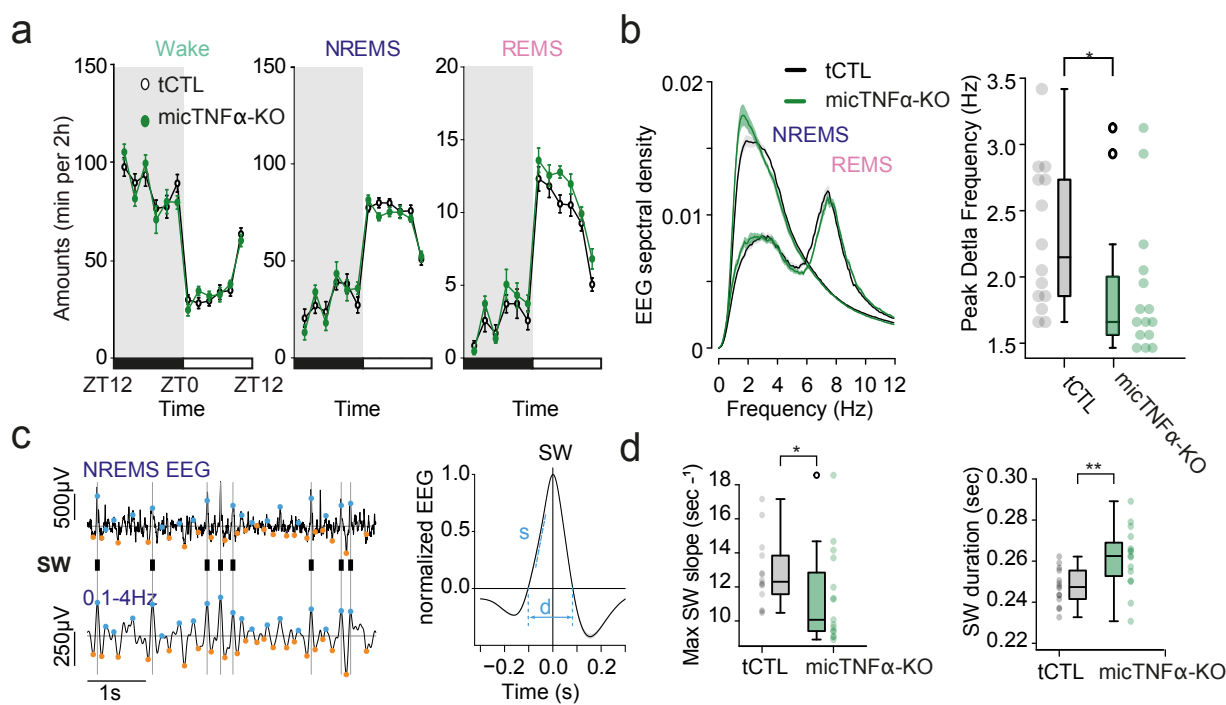


**Fig. 4 - Microglial TNF $\alpha$  modulates slow waves during NREMS.** **a**, Amounts of vigilance states over 24h reported by 2h segments. **b**, Average spectral density (top) of tCTL and micTNF $\alpha$ -KO (lines: means. Shaded area: SEM) and distribution of peak frequency of delta oscillations. The peak delta frequency is significantly lower in micTNF $\alpha$ -KO mice (Mann-Whitney  $W = 157$ ,  $p = 0.025$ ). **c**, Left: Examples of EEG and 0.1-4Hz filtered EEG during NREMS from a transgenic control tCTL; the positive and negative peaks of the delta-filtered signal are indicated by orange and blue points, respectively. Ticks on grey lines indicate large positive deflections corresponding to Slow Waves (SW). Right: average SW for tCTL showing duration (d) and maximum slope (s). **d**, The micTNF $\alpha$ -KO mice exhibit significantly shorter peak onset slope and longer SW duration than tCTL mice. Mann-Whitney  $W=42$   $p=0.005$  and  $W=153$ ,  $p=0.37$  respectively

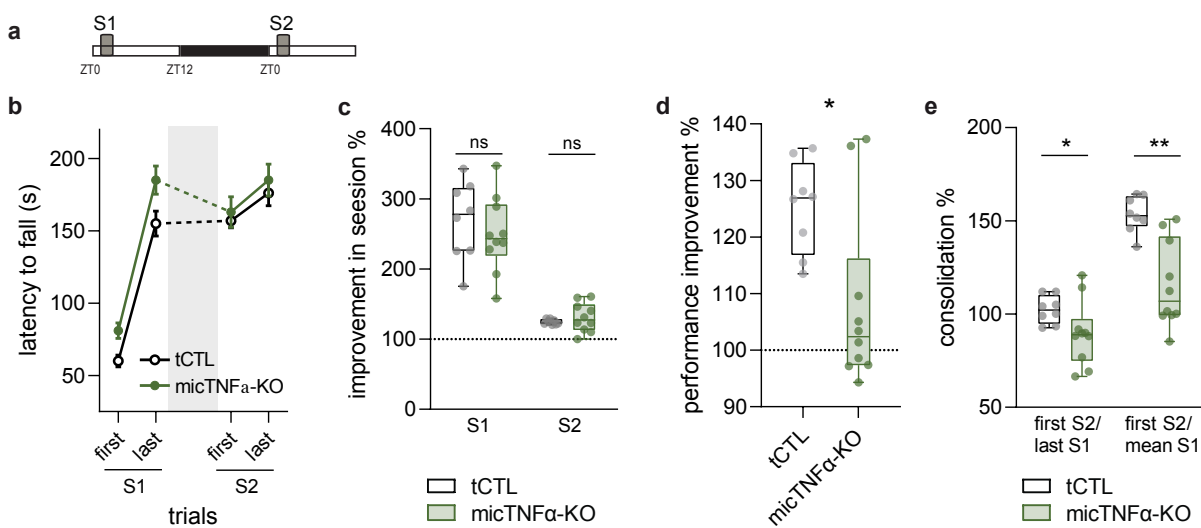


**Fig. 5 – Microglial TNF $\alpha$  required for consolidation of a sleep-dependent motor learning task.** **a**, Experimental design: mice learn to run on the complex wheel (session 1, S1) and consolidation of memory is tested the following day (session 2, S2). Between S1 and S2, mice are left undisturbed in their cages. **b**, Average latency to fall off the complex wheel in the first three and the last three trials of S1 and S2 from tCTL and micTNF $\alpha$ -KO. Grey area represents undisturbed sleep-wake cycle. Dashed line represents S1 to S2 consolidation. **c**, Improvement within each session measured as the ratio between mean of the best three trials and first three trials. **d**, Performance improvement across sessions measured as the ratio between mean of S2 and S1 trials. \*\*\* $p$ <0.001, Mann-Whitney test. **e**, Consolidation of motor learning across sessions measured in two ways: ratio between mean of first 3 trials of S2 and mean of last 3 trials of S1 (first S2/ last S1) or ratio between mean of first 3 trials of S2 and mean of S1 trials (first S2/ mean S1). \* $p$ <0.05 and \*\* $p$ <0.01, Mann-Whitney test. (b-e) 8 tCTL and 10 micTNF $\alpha$ -KO mice.

**Fig. 1 – Plasticity of GABA<sub>A</sub>R in the light/dark cycle is sleep- and microglia-dependent.** **a**, Experimental groups: mice at dark phase (ZT18), mice at light phase (ZT6) and mice submitted to sleep deprivation (dashed) in the light phase (SD6). Vertical bars: time of perfusion. **b**, Representative images showing enrichment of GABA<sub>A</sub>R $\gamma$ 2 (cyan) at cortical L1 inhibitory synapses in the light phase (ZT6). Arrowheads: GABA<sub>A</sub>R $\gamma$ 2 clusters at gephyrin<sup>+</sup>VGAT<sup>+</sup> synapses in control (CTL) or PLX3397-treated mice (PLX). Scale bars, 5 and 1  $\mu$ m. Dashed box corresponds to CTL at ZT18. **c, d**, Mean intensity of GABA<sub>A</sub>R $\gamma$ 2 clusters at gephyrin<sup>+</sup>VGAT<sup>+</sup> synapses (synaptic) and at extrasynaptic sites normalized to ZT18. n= 48 to 65 fields of view (FOVs) from 4-5 mice per group. \*p<0.05, nested t-test; \*\*p<0.01 compared with ZT18 and #p<0.01 compared with SD6, nested one-way ANOVA followed by Sidak's multiple comparison test. **e**, Left: Representative confocal images of VGAT and GABA<sub>A</sub>R $\gamma$ 2 in cortical L5. Yellow line delineates soma identified by NeuN staining. Scale bar, 5  $\mu$ m. Right: Mean intensity of GABA<sub>A</sub>R $\gamma$ 2 at somatic VGAT<sup>+</sup> clusters in L5 normalized to ZT18. n= 60 FOVs from 5 mice per group.

**Fig. 2 – Microglial P2RX7 -TNF $\alpha$  signaling drives GABA<sub>A</sub>Rs synaptic enrichment through CaMKII $\alpha$  phosphorylation.** **a**, Representative confocal images showing increase of GABA<sub>A</sub>R $\alpha$ 1 (cyan) at gephyrin<sup>+</sup> clusters (arrowheads) upon NMDA-induced inhibitory long-term potentiation (iLTP: 2 min 20  $\mu$ M NMDA/10  $\mu$ M CNQX plus 20 min recovery) in organotypic slices cortical L1 (CTL: control; bsl: baseline). **b-e**, Mean intensity of GABA<sub>A</sub>R $\alpha$ 1 clusters at gephyrin<sup>+</sup> cluster normalized to CTL at bsl. n= FOVs/ independent experiments: (b) n= 44 to 69/ 5 to 6; (c) n= 47 to 53/ 5; (d) n= 66 to 102/ 5 to 7; (e) n= 49 to 68/ 7 to 9. \*p<0.05, \*\*p<0.01 and \*\*\*p<0.001, nested one-way ANOVA followed by Sidak's multiple comparison test. iLTP-induced synaptic GABA<sub>A</sub>R enrichment is abolished by: **b**, microglia depletion/inactivation (PLX: PLX3397; SAP: Mac1-saporin; minoc: minocycline); **c**, neutralization of TNF $\alpha$  (nTNF $\alpha$ ); **d**, microglia-specific TNF $\alpha$  deletion through 4-hydroxy-tamoxifen (4-OHT)-induced recombination on CX3CR1<sup>CreERT2/+</sup>:TNF $^{f/f}$  but not on a TNF $^{f/f}$  background; **e**, ATP hydrolysis (apy), P2XR antagonist (PPADS) and P2RX7 antagonist (A74). **f**, Left: Confocal images of GABA<sub>A</sub>R $\alpha$ 1 (cyan) at gephyrin<sup>+</sup> clusters (arrowheads) in bsl and upon BzATP treatment. Right: Mean intensity of GABA<sub>A</sub>R $\alpha$ 1 clusters at gephyrin<sup>+</sup> clusters normalized to CTL at bsl. n= 49 to 63/ 5 to 6. \*p<0.05, \*\*p<0.01, nested one-way ANOVA followed by Sidak's multiple comparison test. **g**, Left: Thr286-phosphorylated CaMKII is enhanced in L1 at the induction phase of plasticity (iLTP0' or BzATP0'). Scale bar, 5  $\mu$ m. Right: Mean intensity of Thr286-phosphorylated CaMKII puncta normalized to bsl. n= 25 to 33 FOVs from 3 independent experiments. \*p<0.05, nested t-test. **h**, Left: Western blot analysis showing iLTP0'-induced CaMKII Thr286-phosphorylation. Right: Ratio between Thr286-phosphorylated CaMKII and total CaMKII normalized to the respective iLTP-free control. n= 5 to 9 independent experiments. \*p<0.05 compared with respective control, Kruskal-Wallis test followed by Dunn's multiple comparisons test. **i**, Model. ATP released downstream NMDA-induced neuronal activity activates microglial P2RX7 with triggers the release of microglial TNF $\alpha$ . TNF $\alpha$  signaling gates CaMKII $\alpha$  autophosphorylation which controls the enrichment of synaptic GABA<sub>A</sub>Rs in pyramidal neurons.

**Fig. 3 – P2RX7 and microglial TNF $\alpha$  promote daily changes in synaptic GABA $A$ R content and CaMKII phosphorylation.** **a**, Representative confocal images of Thr286-phosphorylated CaMKII immunoreactivity in L1 showing higher intensity at ZT6 than ZT18 in transgenic control mice (tCTL). Scale bar, 20  $\mu$ m. **b**, Mean intensity of Thr286-phosphorylated CaMKII signal in L1 normalized to ZT18 for tCTL, microglia-specific TNF $\alpha$  depletion (micTNF $\alpha$ -KO) and P2rx7-KO mice. n= 37 to 50 FOVs from 4-5 mice per group. **c**, Mean intensity of GABA $A$ R $\gamma$ 2 clusters at gephyrin $^+$ VGAT $^+$  synapses normalized to ZT18. n= 48 to 65 FOVs from 4-5 mice per group. \*p<0.05 and \*\*p<0.01, nested t-test.

**Fig. 4 - Microglial TNF $\alpha$  modulates slow waves during NREMS.** **a**, Amounts of vigilance states over 24h reported by 2h segments. Wake, NREMS and REMs are not significantly different between tCTL and micTNF $\alpha$ -KO mice (n=15 mice per group; two-way RM-ANOVA, p=0.1490; p=0.2784, p=0.6838 respectively) **b**, Average spectral density (top) of tCTL and micTNF $\alpha$ -KO (lines: means. Shaded area: SEM) and distribution of peak frequency of delta oscillations. The peak delta frequency is significantly lower in micTNF $\alpha$ -KO mice (Mann-Whitney W = 157, p = 0.025). **c**, Left: Examples of EEG and 0.1-4Hz filtered EEG during NREMS from a transgenic control tCTL; the positive and negative peaks of the delta-filtered signal are indicated by orange and blue points, respectively. Ticks on grey lines indicate large positive deflections corresponding to Slow Waves (SW). Right: average SW for tCTL showing duration (d) and maximum slope (s). **d**, The micTNF $\alpha$ -KO mice exhibit significantly shorter peak onset slope and longer SW duration than tCTL mice. Mann-Whitney W=42 p=0.005 and W=153, p=0.37 respectively.

**Fig. 5 – Microglial TNF $\alpha$  required for consolidation of a sleep-dependent motor learning task.** **a**, Experimental design: mice learn to run on the complex wheel (session 1, S1) and consolidation of memory is tested the following day (session 2, S2). Between S1 and S2, mice are left undisturbed in their cages. **b**, Average latency to fall off the complex wheel in the first three and the last three trials of S1 and S2 from tCTL and micTNF $\alpha$ -KO. Grey area represents undisturbed sleep-wake cycle. Dashed line represents S1 to S2 consolidation. **c**, Improvement within each session measured as the ratio between mean of the best three trials and first three trials. **d**, Performance improvement across sessions measured as the ratio between mean of S2 and S1 trials. \*\*\*p<0.001, Mann-Whitney test. **e**, Consolidation of motor learning across sessions measured in two ways: ratio between mean of first 3 trials of S2 and mean of last 3 trials of S1 (first S2/ last S1) or ratio between mean of first 3 trials of S2 and mean of S1 trials (first S2/ mean S1). \*p<0.05 and \*\*p<0.01, Mann-Whitney test. (b-e) 8 tCTL and 10 micTNF $\alpha$ -KO mice.